

Title	Low temperature germanium to silicon direct wafer bonding using free radical exposure
Authors	Byun, Ki Yeol;Ferain, Isabelle;Fleming, Peter G.;Morris, Michael A.;Goorsky, M. S.;Colinge, Cindy
Publication date	2010
Original Citation	Byun, K. Y., Ferain, I., Fleming, P., Morris, M., Goorsky, M. and Colinge, C. (2010) 'Low temperature germanium to silicon direct wafer bonding using free radical exposure', Applied Physics Letters, 96(10), pp. 102110. doi: 10.1063/1.3360201
Type of publication	Article (peer-reviewed)
Link to publisher's version	<a href="http://aip.scitation.org/doi/abs/10.1063/1.3360201">http://aip.scitation.org/doi/abs/10.1063/1.3360201</a> - 10.1063/1.3360201
Rights	© 2010 American Institute of Physics.This article may be downloaded for personal use only. Any other use requires prior permission of the author and AIP Publishing. The following article appeared in Byun, K. Y., Ferain, I., Fleming, P., Morris, M., Goorsky, M. and Colinge, C. (2010) 'Low temperature germanium to silicon direct wafer bonding using free radical exposure', Applied Physics Letters, 96(10), pp. 102110 and may be found at <a href="http://aip.scitation.org/doi/abs/10.1063/1.3360201">http://aip.scitation.org/doi/abs/10.1063/1.3360201</a>
Download date	2023-05-07 14:21:53
Item downloaded from	<a href="http://hdl.handle.net/10468/4344">http://hdl.handle.net/10468/4344</a>



# UCC

**University College Cork, Ireland**  
Coláiste na hOllscoile Corcaigh

# Low temperature germanium to silicon direct wafer bonding using free radical exposure

Ki Yeol Byun<sup>\*</sup>, Isabelle Ferain, Pete Fleming, Michael Morris, Mark Goorsky, and Cindy Colinge

Citation: *Appl. Phys. Lett.* **96**, 102110 (2010); doi: 10.1063/1.3360201

View online: <http://dx.doi.org/10.1063/1.3360201>

View Table of Contents: <http://aip.scitation.org/toc/apl/96/10>

Published by the [American Institute of Physics](#)

---

## Articles you may be interested in

[Surface activated bonding of silicon wafers at room temperature](#)  
*Applied Physics Letters* **68**, 2222 (1998); 10.1063/1.115865

[Silicon-to-silicon direct bonding method](#)  
*Journal of Applied Physics* **60**, 2987 (1998); 10.1063/1.337750

[Mechanisms for room temperature direct wafer bonding](#)  
*Journal of Applied Physics* **113**, 094905 (2013); 10.1063/1.4794319

---



# Low temperature germanium to silicon direct wafer bonding using free radical exposure

Ki Yeol Byun,<sup>1,a)</sup> Isabelle Ferain,<sup>1</sup> Pete Fleming,<sup>2</sup> Michael Morris,<sup>1,3</sup> Mark Goorsky,<sup>4</sup> and Cindy Colinge<sup>1</sup>

<sup>1</sup>Tyndall National Institute, University College Cork, Lee Maltings, Cork, Ireland

<sup>2</sup>Environmental Research Institute, University College Cork, Cork, Ireland

<sup>3</sup>Department of Chemistry, University College Cork, Cork, Ireland

<sup>4</sup>Department of Material Science and Engineering, UCLA, California 90095, USA

(Received 18 December 2009; accepted 19 February 2010; published online 12 March 2010)

A low temperature germanium (Ge) to silicon (Si) wafer bonding method was demonstrated by *in situ* radical activation bonding in vacuum. In order to gain further insight into the bonding mechanism, the Ge surface chemistry after either oxygen or nitrogen radical activation was analyzed by means of angle-resolved x-ray photoelectron spectroscopy. After low temperature direct bonding of Ge to Si followed by annealing at 200 and 300 °C, advanced imaging techniques were used to characterize the bonded interface. © 2010 American Institute of Physics. [doi:10.1063/1.3360201]

Germanium is a candidate to replace Si in the channel of future high performance p-channel metal-oxide semiconductor field effect transistor devices due to its high mobility transport properties.<sup>1</sup> In that respect, the germanium on insulator (GeOI) configuration is attractive as it facilitates carrier transport and has reduced junction leakage currents.<sup>2,3</sup> Preparing GeOI made via Ge condensation methodologies presents considerable challenges as undesirable over-oxidation or high stacking fault concentrations in interfaces.<sup>4</sup>

Ge to Si direct wafer bonding has been studied for use in high-performance photodetectors as well as high-quality epitaxial templates for GaAs growth.<sup>5</sup> However, Ge to Si bonding poses a challenge since the coefficient of thermal expansion (CTE) mismatch.<sup>6</sup> Little attention has been dedicated to the chemical and structural investigations of the bonded Ge to Si interface.

The effects of free radical activation for Si to Si bonding have been previously reported by our group.<sup>7</sup> In this letter, we focus on the characterization of activated Ge surfaces using oxygen and nitrogen radicals and show low temperature Ge to Si direct bonding using radical activation. The chemical species on the activated Ge surfaces were investigated using angle-resolved x-ray photoelectron spectroscopy (ARXPS), while structural analysis was performed by scanning acoustic microscopy (SAM), and high-resolution transmission electron microscopy (HR-TEM).

In the experiment, 4 in. (100) oriented p-type Ge (Ga doped, resistivity=0.016 Ω cm) were selected for ARXPS analysis. The oxygen and nitrogen radical activated Ge surfaces were studied in a Vacuum Science Workshop Atomtech ESCA system using Al K $\alpha$  radiation (1486.6 eV). The Ge wafers were cleaned in an SC1-equivalent solution without ozone using a Semitool Spray Acid Tool prior to activation. Wafers were then loaded into Applied Microengineering Limited (AML) AW04 bonder and vacuum was applied. The wafers were then exposed for 10 min to either oxygen or nitrogen free radicals generated by a remote plasma ring. A reference sample of Ge cleaned and bonded without exposure was also prepared. Wafers were bonded under a pressure

of 1 kN applied for 5 min and immediately transferred for XPS analysis. The three bonded Ge to Ge samples were then debonded using a razor blade, cleaved into 2×2 cm<sup>2</sup> size and loaded into a high vacuum sample holder. The photoelectron peaks and chemical composition of the Ge surface were analyzed at various take-off angles.<sup>8</sup>

In the next experiment, blank Ge wafers were bonded directly to Si using the same recipe used for the Ge bonded to Ge. 4 in. (100)-oriented n-type prime grade bare Si wafers were bonded with the Ge wafers. Prior to bonding, the Ge and Si wafers were cleaned in an SC1-equivalent solution with ozone for Si and without ozone for Ge. After loading into the AML wafers were activated and bonded *in situ* under a pressure of 1 kN applied for 5 min at a chamber pressure of 10<sup>-5</sup> mbar. The wafers were annealed *in situ* at 100 °C for 1 h with an applied pressure of 500 N in vacuum followed by an *ex situ* anneal at 200 °C for 24 h and additionally 300 °C for 24 h. The ramp-up rate was set to 0.5 °C/min in both cases. After anneal, Ge–Si bonded pairs were remained intact despite the CTE mismatch. The bond strength of the bonded pairs was measured using the crack opening method combined with SAM. Structural analysis of buried interfaces was studied by SAM and HR-TEM.

Binding state configurations of Ge atoms at the activated surfaces were evaluated by ARXPS using the debonded cleaved samples. Figure 1 shows the Ge 2p<sub>3/2</sub>, Ge 3d photoelectron features (take-off angle=75°). As expected the Ge 2p<sub>3/2</sub> signal shows two binding energy contributions at 1218.5 and 1221.0 (+/-0.2) eV.<sup>9</sup> These can be assigned to zero-valent and quadravalent germanium, respectively. Zero-valent corresponds to bulk Ge while quadravalent indicates the presence of GeO<sub>2</sub>. The Ge 3d peaks exhibit similar information. Two features can be resolved at 29.8 and 32.5 eV that once again are assignable to zero-valent and quadravalent Ge, respectively.<sup>10</sup> There was no evidence in this work of the formation of detectable quantities of substoichiometric oxides.

Quantitative relative contributions of the oxygen and Ge features are found by curve-fitting the XPS data. These data are reported in Table I as peak area ratios and are used to derive stoichiometric amounts using known sensitivity

<sup>a)</sup>Electronic mail: kiyeol.byun@tyndall.ie.

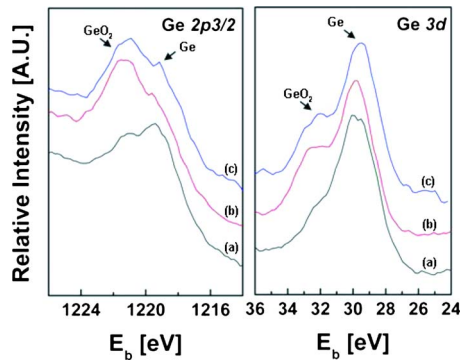


FIG. 1. (Color online) Ge  $2p_{3/2}$  and Ge  $3d$  photoelectron features (take-off angle =  $75^\circ$ ): (a) reference cleaned sample, (b) oxygen radical activated sample, and (c) nitrogen radical activated sample.

factors.<sup>11</sup> The data collected at  $75^\circ$  is the most accurate representation of the actual stoichiometry close to the Ge surface.

Curve fitting reveals a peak signifying the presence of  $\text{OH}^-$  which is located at a higher binding energy than the binding energy of  $\text{GeO}_2$ .<sup>12</sup> This data is shown in the first column of Table I where the ratio of  $\text{OH}^-$  to  $\text{GeO}_2$  (labeled  $\text{O}^-/\text{O}^{2-}$ ) is represented. In the second column we have derived the O/Ge ratio which is the total O  $1s$  peak area divided by total Ge  $2p_{3/2}$  peak area. From the second column of Table I, it is clear that exposure of hydrophilic cleaned Ge substrates to free radicals produces some oxidation at low temperature free radical exposure.

For both the nitrogen and oxygen radical exposed samples the quantification shown in Table I shows higher values of O/Ge ratio, which is more likely due to a thicker oxide film compared to the reference Ge sample. The nitrogen radical exposed Ge also shows a significant  $\text{GeO}_2$  formation; this is similar to previous studies where Ge exposed to nitrogen plasma resulted in a more hydrophilic surface signifying formation of an oxide.<sup>13</sup> These quantifiable XPS data were used to estimate the film thickness as 0.39, 0.58, and 0.72 nm for the reference, nitrogen radical activated and oxygen radical activated samples, respectively.<sup>8</sup>

Most extensive hydroxylation, which is indicated in the first column of Table I, was observed for the reference samples. Nitrogen radical activated samples gave the lowest

TABLE I. ARXPS peak area ratio.  $\text{O}^-/\text{O}^{2-}$  is the  $\text{O}^-$  signal area divided by  $\text{O}^{2-}$  signal area in O  $1s$  spectra. O/Ge is the total O  $1s$  peak area divided by total Ge  $2p_{3/2}$  peak area.

Sample	Take-off angle (deg)	$\text{O}^-/\text{O}^{2-}$	O/Ge Total
Reference substrate	0	0.34	0.04
	25	0.24	0.04
	50	0.09	0.08
	75	0.00	0.25
Post oxygen radical	0	0.11	0.06
	25	0.11	0.07
	50	0.02	0.12
	75	0.00	0.40
Post nitrogen radical	0	0.07	0.05
	25	0.09	0.06
	50	0.06	0.11
	75	0.00	0.35

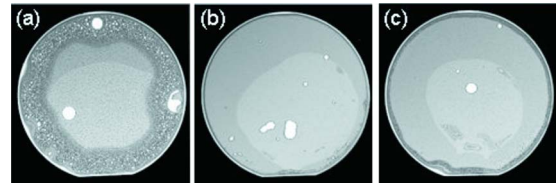
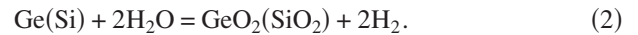
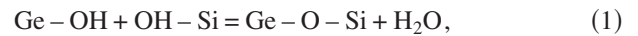


FIG. 2. (Color online) SAM images of Ge/Si bonded wafer pairs after annealing at  $200^\circ\text{C}$  for 24 h, and additionally at  $300^\circ\text{C}$  for 24 h: (a) cleaned in an SC1-equivalent solution, followed by (b) oxygen radical 10 min exposure, and (c) nitrogen radical 10 min exposure.

$-\text{OH}$  concentration and oxygen radical activated samples an intermediate value. The presence of hydroxyl species is important because increased hydroxyl groups can give rise to more hydrophilic reactions at bonded interfaces, which can then induce intrinsic void generation due to trapped reaction by-products.

Figure 2 shows SAM images of bonded pairs after annealing at  $200^\circ\text{C}$  24 h and additionally at  $300^\circ\text{C}$  for 24 h; (a) precleaned by SC1-equivalent solution, (b) post oxygen radical exposure, and (c) post nitrogen radical exposure. The hydrophilic reaction at the interfaces can be described using Eqs. (1) and (2).



The interface reaction creates trapped gas (water vapor or hydrogen) following the hydrophilic chemical reaction. Trapped by-products appear as a different contrast in the SAM images. Some of the water molecules resulting from covalent bonding of  $\text{Ge}-\text{O}-\text{Si}$  can diffuse through the nanometer range oxide layer and react with the bulk Ge and Si to form dioxide and hydrogen. In Fig. 2(a), however, the buried oxide is so thin that the reactants and by-products cannot diffuse from the interface. Radical activated samples in Figs. 2(b) and 2(c), show minimal intrinsic voids due to the ability of the relatively thick oxide interface to enhance by-product diffusion. The nitrogen radical activated sample in Fig. 2(c), has a thinner oxide than the oxygen radical activated sample [Fig. 2(b)], and therefore there is some void generation seen near the wafer edge. Void formation during low temperature anneal depends on the thickness of the stoichiometric oxide film, which is consistent with Si bonding.<sup>14</sup> The SAM images which show the reference sample (thinnest oxide) with the most intrinsic voids, followed by nitrogen activated sample (intermediate oxide thickness) and then the oxygen activated sample (thickest oxide) agrees with the oxide thickness values extracted from ARXPS.

Table II shows the bond strength as a function of the stoichiometric oxide film thickness which depends on activation conditions. The bonding energy ( $\text{mJ}/\text{m}^2$ ) is calculated by using the following equation:<sup>15</sup>

TABLE II. Bond strength for wafer pairs at different activation conditions. Wafers were annealed at  $200^\circ\text{C}$  for 24 h, and additionally at  $300^\circ\text{C}$  for 24 h.

Activation	Reference	Nitrogen radical	Oxygen radical
Bond strength ( $\text{mJ}/\text{m}^2$ )	489	676	911

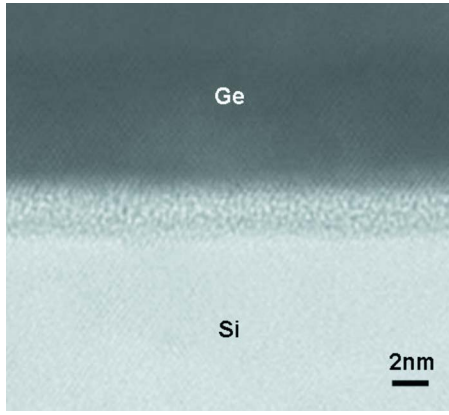


FIG. 3. (Color online) HR-TEM observation of buried interfaces after annealing at 200 °C for 24 h and additional 300 °C for 24 h.

$$\gamma = \frac{3t_b^2 E_1 t_{w1}^3 E_2 t_{w2}^3}{8L^4 (E_1 t_{w1}^3 + E_2 t_{w2}^3)}, \quad (3)$$

where  $E_1$  and  $E_2$  are Young's modulus for Si ( $1.66 \times 10^{11}$  Pa) and Ge ( $1.03 \times 10^{11}$  Pa), respectively,  $t_b$  is the blade thickness,  $t_{w1}$  is the Si wafer thickness,  $t_{w2}$  is the Ge wafer thickness, and  $L$  is the crack propagation length. The oxygen radical activated sample shows the highest bond strength.

Figure 3 shows cross-sectional HR-TEM image of buried interfaces using oxygen radical activation after 200 °C and an additional 300 °C 24 h anneal. The 2-nm-thick buried interface appears defect-free and a smooth bonded interface is visible. Additionally, compared to the Ge condensation technique,<sup>4</sup> the TEM image shows no over oxidation or stacking faults generated during the low thermal budget ( $\leq 300$  °C) anneal.

Radical activation can enhance the bonding reaction allowing strong bond strength at low temperature while pre-

serving the crystalline quality of the Ge. Additional experiments are required to fully characterize the electrical properties in interfaces.

This work was supported by the Science Foundation Ireland Grant No. 07/IN/I937; Low Temperature Wafer Bonding for Heterogeneous Integration. This work has also been enabled by the Science Foundation Ireland Grant No. 08/W.1/I2597; Heterogeneous materials integration for III-V optoelectronics and solar cell applications.

<sup>1</sup>C. Chui, H. Kim, D. Chi, B. Triplett, P. McIntyre, and K. Saraswat, Tech. Dig. - Int. Electron Devices Meet. **2002**, 437.

<sup>2</sup>T. Akatsu, C. Deguet, L. Sanchez, F. Allibert, D. Rouchon, T. Signamarcheix, C. Richtarch, A. Boussagol, V. Loup, F. Mazen, J. Hartmann, Y. Campidelli, L. Clavelier, F. Letertre, N. Kernevez, and C. Mazure, *Mater. Sci. Semicond. Process.* **9**, 444 (2006).

<sup>3</sup>Q. Nguyen, J. Damlencourt, B. Vincent, L. Clavelier, Y. Morand, P. Gentil, and S. Cristoloveanu, *Solid-State Electron.* **51**, 1172 (2007).

<sup>4</sup>T. Tezuka, Y. Moriyama, S. Nakaharai, N. Sugiyama, N. Hirashita, E. Toyoda, Y. Miyamura, and S. Takagi, *Thin Solid Films* **508**, 251 (2006).

<sup>5</sup>L. Chen, P. Dong, and M. Lipson, *Opt. Express* **16**, 11513 (2008).

<sup>6</sup>M. Kim and R. Carpenter, *J. Electron. Mater.* **32**, 849 (2003).

<sup>7</sup>K. Byun, I. Ferain, and C. Colinge, *J. Electrochem. Soc.* **157**, H109 (2010).

<sup>8</sup>J. Watts and J. Wolstenholme, *An Introduction to Surface Analysis by XPS and AES* (Wiley, New York, 2003).

<sup>9</sup>B. Pelissier, H. Kambara, E. Godot, E. Veran, V. Loup, and O. Joubert, *Microelectron. Eng.* **85**, 151 (2008).

<sup>10</sup>A. Molle, M. Bhuiyan, G. Tallarida, and M. Fanciulli, *Appl. Phys. Lett.* **89**, 083504 (2006).

<sup>11</sup>M. Seah, I. Gilmore, and S. Spencer, *J. Electron Spectrosc. Relat. Phenom.* **120**, 93 (2001).

<sup>12</sup>W. Ranke, *J. Electron Spectrosc. Relat. Phenom.* **61**, 231 (1993).

<sup>13</sup>X. Ma, C. Chen, W. Liu, X. Liu, X. Du, Z. Song, and C. Lin, *J. Electrochem. Soc.* **156**, H307 (2009).

<sup>14</sup>S. Vincent, I. Radu, D. Landru, F. Leterte, and F. Rieutord, *Appl. Phys. Lett.* **94**, 101914 (2009).

<sup>15</sup>Q.-Y. Tong and U. Gösele, *Semiconductor Wafer Bonding: Science and Technology* (Wiley, New York, 1999), p. 28.